Letter

Thermal drag effect in quantum Hall circuits

Edvin G. Idrisov *
Department of Physics and Materials Science, University of Luxembourg, L-1511 Luxembourg, Luxembourg

Ivan P. Levkivskyi
Dropbox Ireland, One Park Place, Hatch Street Upper, Dublin D02FD79, Ireland

Eugene V. Sukhorukov
Département de Physique Théorique, Université de Genève, CH-1211 Genève 4, Switzerland

(Received 15 March 2022; revised 21 July 2022; accepted 21 September 2022; published 30 September 2022)

We study the thermal drag between two mesoscopic quantum Hall (QH) circuits. Each circuit consists of an ohmic contact perfectly coupled to quantum Hall edge states. The drag is caused by strong capacitive coupling between ohmic contacts. The nonequilibirum conditions and the electron-electron interaction are considered by using the bosonization technique in the combination with the scattering theory or, equivalently, with the help of the Langevin equations. The thermal drag current in the passive circuit, the noise power of the corresponding heat current, and the Fano factor are calculated and analyzed for different coupling strengths.

DOI: 10.1103/PhysRevB.106.L121405

I. INTRODUCTION

The mutual electron drag effect is the phenomenon that arises in a system of two isolated (in the absence of the transfer of charge) quantum circuits coupled via the long-range Coulomb interaction [1]. Typically, one is interested in the so-called Coulomb drag effect, where the charge current in the active part of the circuit causes the charge drag current in the passive part of the circuit [2], and normally, this effect is perturbative and weak. The Coulomb drag effect in various systems was thoroughly studied both experimentally and theoretically [1]. It was further shown that the charge drag current can also be mediated by the combined electron-phonon, electron-photon, and electron-ion interactions [3–5]. All these effects must be differentiated from the thermal drag effect, which can also be caused by the long-range Coulomb interaction [6–9]. In this case, the flow of heat current in the active circuit results in the heat current in the passive circuit. Of particular interest is the thermal drag effect due to the temperature difference between active and passive circuits. The effect of thermal drag was studied in the context of quantum refrigerators and engines, heat diodes, and heat pumps [10–15].

The recent progress in the fabrication of hybrid systems that are based on chiral quantum Hall (QH) edge states made it possible to do accurate mesoscopic experiments with strongly interacting electron systems [16]. An interesting example of such a system is a QH edge state perfectly coupled to an ohmic contact, a mesoscale metallic granula with negligible level spacing and finite charging energy comparable with the temperature [17]. It is worth mentioning that such an ohmic contact immediately became a key element of experimental and theoretical studies [16], remarkable examples being the suppression of charge quantization caused by quantum and thermal fluctuations [18,19], the heat Coulomb blockade effect [20–22], the interaction-induced recovery of the phase coherence [23–25], the charge Kondo effect [26,27], the quantization of the anyonic heat flow [28], and the observation of the half-integer thermal Hall conductance [29,30].

In this letter, we propose a mesoscopic QH system with embedded ohmic contacts, building up strong Coulomb interactions, for studying the thermal drag effect (see Fig. 1). The system consists of the active (upper) and passive (lower) quantum circuits. Each circuit includes an ohmic contact perfectly coupled to a chiral QH edge state: The edge state enters an ohmic contact and leaves it without electron backscattering. The thermal drag effect is caused by the capacitive coupling between ohmic contacts of the active and passive circuits. The temperature difference $T_{\mathrm{in,u}} - T_{\mathrm{in,d}} > 0$ is applied between circuits which causes the temperature imbalance between contacts and results in the thermal heat flow from the upper to the lower part. We assume the full thermalization of the electron systems inside ohmic contacts and find their temperatures for the energy balance equations. In this letter, we focus on the thermal drag current, its zero-frequency noise power, and the associated Fano factor. The bosonization technique in combination with the scattering theory for bosons allows us to account for the strong interactions nonperturbatively. Recent experimental studies of systems with one ohmic contact coupled to edge channels [16–18,25–30] and with two coupled ohmic contacts [31] demonstrate the experimental feasibility of our proposal. The temperatures of the experiments have to be compared with the charging energies of ohmic contacts. In all these experiments, micron-sized ohmic contacts were used. This is a sufficient condition for the strong interaction effects to be observed.

*idrisoft@gmail.com

 ©2022 American Physical Society

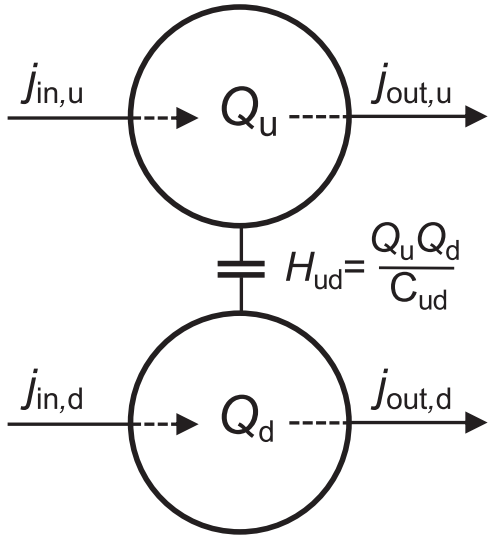

FIG. 1. Schematic of the possible experimental setup. The systems consists of two identical quantum circuits: upper (active) and lower (passive) parts. Each part includes an ohmic contact (metallic granula with capacitance C and negligible level spacing) which is perfectly coupled to a chiral integer quantum Hall (QH) channel (the channel enters an ohmic contact and leaves it without electron backscattering). The incoming channels are kept at different temperatures $T_{\mathrm{in,u}} - T_{\mathrm{in,d}} > 0$. The capacitive coupling between ohmic contacts $Q_{\mathrm{u}}Q_{\mathrm{d}}/C_{\mathrm{ud}}$ results in thermal drag effect: The upper mesoscopic circuit induces extra heat current in the lower circuit in the outgoing channel.

II. MODEL AND THEORETICAL APPROACH

We use the low-energy effective field theory [32,33] to describe QH edge states strongly coupled to the ohmic contacts. The ohmic contact is modeled by extending an edge state inside the metallic granula and splitting it into two uncorrelated channels [20,21]. The Hamiltonian of each quantum circuit

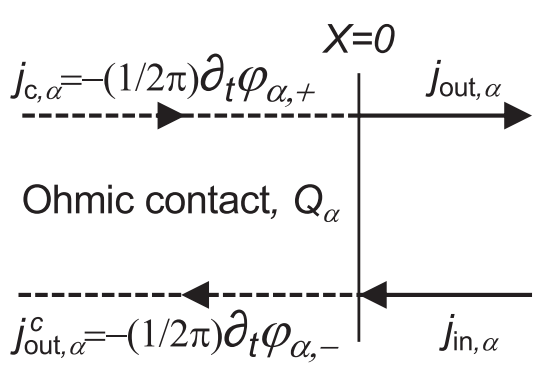

FIG. 2. The model of an ohmic contact with the capacitive interaction is illustrated, see Eq. (1). The charge current $j_{\mathrm{in},\alpha}(t)$ arriving at the ohmic contact enters it at the interface at $x = 0$ and continues as a neutral current $j^{\mathrm{c}}_{\mathrm{out},\alpha}(t)$. The neutral current $j^{\mathrm{c}}_{\alpha}(t)$ arriving at the interface from inside the ohmic contact continues as a charge current $j_{\mathrm{out},\alpha}(t)$. To account for the negligible level spacing in the ohmic contact, we extend edge states inside it to minus infinity and introduce the small regularization parameter ϵ in Eq. (1).

($\alpha = \mathrm{u}, \mathrm{d}$) contains two terms (see Fig. 2):

$$H_\alpha = \frac{v_F}{4\pi}\sum_{\sigma=\pm}\int dx(\partial_x\phi_{\alpha\sigma})^2 + \frac{Q_\alpha^2}{2C},$$
$$Q_\alpha = \int_{-\infty}^{0} dx \exp\left(\frac{\epsilon x}{v_{\mathrm{F}}}\right)[\rho_{\alpha+}(x) + \rho_{\alpha-}(x)], \tag{1}$$

where v_{F} is the Fermi velocity, C is the capacitance of each ohmic contact, Q_α is an operator of the total charge accumulated at each ohmic contact, and ϵ is a small regularization parameter. Here, the first term accounts for the dynamics of incoming and outgoing edge channels, and the second term describes the charging energy of an ohmic contact of a finite size. The set of scalar fields $\phi_{\alpha\sigma}(x,t)$, where $\alpha = \mathrm{u}, \mathrm{d}$ and $\sigma = \pm$, are introduced in Eq. (1) to describe the low-energy physics. The operators of edge charge densities and currents for incoming $\sigma = -$ and outgoing $\sigma = +$ states are given by $\rho_{\alpha\sigma} = (1/2\pi)\partial_x\phi_{\alpha\sigma}$ and $j_{\alpha\sigma} = -(1/2\pi)\partial_t\phi_{\alpha\sigma}$. The bosonic fields satisfy the standard canonical commutation relations:

$$[\partial_x\phi_{\alpha\sigma}(x,t), \phi_{\alpha'\sigma'}(x',t)] = 2\pi i\sigma\delta_{\alpha\alpha'}\delta_{\sigma\sigma'}\delta(x-x'), \tag{2}$$

where $\delta_{\alpha\alpha'}$ is the Kronecker delta, and $\delta(x)$ is the Dirac delta function. It is worth mentioning that the model presented above of an ohmic contact was successfully used to explained the experiments on the charge quantization, heat Coulomb blockade, and heat quantization of anyonic flow [18,22,25].

The total Hamiltonian of the system includes three terms (see Fig. 1):

$$H = H_{\mathrm{u}} + H_{\mathrm{d}} + H_{\mathrm{ud}}, \tag{3}$$

where the Hamiltonians of the active and passive circuit H_α are given in Eq. (1), while capacitive coupling between ohmic contacts has the form:

$$H_{\mathrm{ud}} = \frac{Q_{\mathrm{u}}Q_{\mathrm{d}}}{C_{\mathrm{ud}}}, \tag{4}$$

where $1/C_{\mathrm{ud}}$ is the mutual capacitive coupling constant.

Using commutation relations in Eq. (2), the Hamiltonians in Eqs. (1) and (3), and the boundary conditions for the fields in terms of incoming and outgoing currents $\partial_t\phi_{\alpha+}(-\infty,t) = -2\pi j_{\mathrm{c},\alpha}(t)$, $\partial_t\phi_{\alpha+}(0,t) = -2\pi j_{\mathrm{out},\alpha}(t)$, $\partial_t\phi_{\alpha-}(0,t) = -2\pi j_{\mathrm{in},\alpha}(t)$, and $\partial_t\phi_{\alpha-}(-\infty,t) = -2\pi j^{\mathrm{c}}_{\mathrm{out},\alpha}(t)$, one can write and solve the equations of motion for the fields. Here, $j_{\mathrm{in},\alpha}(t)$ is the incident charged current flowing toward the ohmic contact α, the current $j_{\mathrm{c},\alpha}(t)$ describes the neutral mode that originates from the ohmic contact α and acquires its temperature $T_{\mathrm{c},\alpha}$, the current $j^{\mathrm{c}}_{\mathrm{out},\alpha}(t)$ is the outgoing neutral mode propagating toward deep inside the ohmic contact α, and finally, $j_{\mathrm{out},\alpha}(t)$ is the outgoing charged current propagation from the ohmic contact α (see Fig. 2).

On one hand, the equations of motion for the currents and the charges can be presented in a form of Langevin equations [19,21], namely,

$$\partial_t Q_\alpha(t) = j_{\mathrm{in},\alpha}(t) - j_{\mathrm{out},\alpha}(t),$$
$$j_{\mathrm{out},\alpha}(t) = \frac{Q_\alpha(t) + \lambda Q_{-\alpha}(t)}{\tau_{\mathrm{c}}} + j_{\mathrm{c},\alpha}(t), \tag{5}$$
$$j_{\mathrm{out},\alpha}(t) + j^{\mathrm{c}}_{\mathrm{out},\alpha}(t) = j_{\mathrm{in},\alpha}(t) + j_{\mathrm{c},\alpha}(t),$$

where $\lambda = C/C_{\rm ud} \leqslant 1$ is the dimensionless coupling constant, $\tau_{\rm c} = R_{\rm q}C$ is the charge relaxation time, $R_{\rm q} = 2\pi\hbar/e^2$ is the resistance quantum, and the notation $-\alpha = {\rm d}, {\rm u}$ indicates swapping the indexes $\alpha = {\rm u}, {\rm d}$. Here, the first equation expresses the conservation of charge in the circuit α. The second line is the Langevin equation, which has the simple meaning: The outgoing current acquires one contribution $[Q_\alpha(t) + \lambda Q_{-\alpha}(t)]/\tau_{\rm c}$ from the time-dependent potential of an ohmic contact α and the second contribution $j_{{\rm c},\alpha}$ that can be viewed as a Langevin source. The third equation expresses the conservation of the total particle current separately in the upper and lower circuits.

On the other hand, the equations of motion with open boundary conditions can also be used to formulate the scattering theory and relate four outgoing and four incoming currents with the unitary scattering matrix:

$$\mathbf{J}_{\rm out}(\omega) = \hat{\mathcal{U}}(\omega)\mathbf{J}_{\rm in}(\omega), \tag{6}$$

where $\mathbf{J}_{\rm out} = (j_{\rm out,u}, j_{\rm out,d}, j^{\rm c}_{\rm out,u}, j^{\rm c}_{\rm out,d})$, and $\mathbf{J}_{\rm in} = (j_{\rm in,u}, j_{\rm in,d}, j_{\rm c,u}, j_{\rm c,d})$. The scattering matrix in Eq. (6) has the form:

$$\hat{\mathcal{U}}(\omega) = \begin{bmatrix} \mathcal{A} & \mathcal{B} & \mathcal{C} & -\mathcal{B} \\ \mathcal{B} & \mathcal{A} & -\mathcal{B} & \mathcal{C} \\ \mathcal{C} & -\mathcal{B} & \mathcal{A} & \mathcal{B} \\ -\mathcal{B} & \mathcal{C} & \mathcal{B} & \mathcal{A} \end{bmatrix}, \tag{7}$$

where $\mathcal{A}(\omega) = [i\omega\tau_{\rm c} + \lambda^2 - 1]/[(\omega\tau_{\rm c} + i)^2 + \lambda^2]$, $\mathcal{B}(\omega) = i\lambda\omega\tau_{\rm c}/[(\omega\tau_{\rm c} + i)^2 + \lambda^2]$, and $\mathcal{C}(\omega) = \omega\tau_{\rm c}[\omega\tau_{\rm c} + i]/[(\omega\tau_{\rm c} + i)^2 + \lambda^2]$. One can easily check the unitary $\hat{\mathcal{U}}^\dagger(\omega) = \hat{\mathcal{U}}(\omega)^{-1}$, which reflects the conservative character of the equations of motion, before Langevin sources are traced out. It is also worth mentioning that, at $\lambda = 0$ or 1, one recovers the results for the scattering matrix obtained in Refs. [19,21,24].

Next, let us recall that currents originating from ohmic contacts are in equilibrium. Thus, the two-point correlation functions of the incoming currents as well as the Langevin sources are given by the equilibrium spectral function [34]:

$$\langle j_{l,\alpha}(\omega) j_{k,\beta}(\omega')\rangle = 2\pi\delta_{lk}\delta_{\alpha\beta}\delta(\omega + \omega')R_{\rm q}^{-1}S_{l,\alpha}(\omega), \tag{8}$$

where $S_{l,\alpha}(\omega) = \omega/[1 - \exp(-\omega/T_{l,\alpha})]$, $l, k = {\rm in}, {\rm c}$, and $\alpha, \beta = {\rm u}, {\rm d}$. These correlation functions are used for further calculations. Note that the temperatures of ohmic contacts $T_{\rm c,u/d}$ are yet to be found from the energy balance equations.

III. HEATING EFFECT AND THERMAL DRAG CURRENT

In a chiral QH channel, the energy current operator is equal to the energy density operator multiplied by group velocity $\mathcal{J}_{l,\alpha}(t) = (v^2/4\pi)[\partial_x\phi_{l,\alpha}(x,t)]^2$. Using the equation of motion for the bosonic field $\phi_{l,\alpha}(x,t)$, one can rewrite the energy current as $\mathcal{J}_{l,\alpha}(t) = (R_{\rm q}/2)j^2_{l,\alpha}(t)$, where $j_{l,\alpha}(t)$ are given in Eqs. (5) and (6). The heat current can be obtained by subtracting the vacuum (zero temperature) contribution:

$$J_{l,\alpha} = \frac{R_{\rm q}}{2}\left[\langle j^2_{l,\alpha}\rangle - \langle j^2_{l,\alpha}\rangle_{\rm vac}\right]. \tag{9}$$

For a ballistic equilibrium channel at the filling factor $\nu = 1$ and temperature T, one uses the noise spectral function in Eq. (8) to arrive at the known result [21,35]: $J = \pi k_{\rm B}^2 T^2/12\hbar \equiv J_{\rm Q}$, where J_Q is called the heat flux quantum.

Next, to find temperatures $T_{\rm c,u}$ and $T_{\rm c,d}$ in Eq. (8), we solve self-consistently the energy balance equations, i.e., the conservation of incoming and outgoing heat currents at the ohmic contacts (coupling to phonons, neglected here, can be considered as in Ref. [22,36]). These equations read $J_{\rm c,u} = J^{\rm c}_{\rm out,u}$, $J_{\rm c,d} = J^{\rm c}_{\rm out,d}$, where the heat currents are defined in Eq. (9). Using the relations between incoming and outgoing currents in Eq. (6) and spectral noise functions from the Eq. (8), one arrives at the system of coupled nonlinear equations for temperatures of ohmic contacts:

$$\begin{aligned} \frac{\pi T^2_{\rm c,u}}{12} &= \frac{\pi T^2_{\rm in,u}}{12} + J^{\mathcal{B}}_{\substack{\rm in,d\\ \rm in,u}}(\lambda) + J^{\mathcal{A}}_{\substack{\rm c,u\\ \rm in,u}}(\lambda) + J^{\mathcal{B}}_{\substack{\rm c,d\\ \rm in,u}}(\lambda), \\ \frac{\pi T^2_{\rm c,d}}{12} &= \frac{\pi T^2_{\rm in,d}}{12} + J^{\mathcal{B}}_{\substack{\rm in,u\\ \rm in,d}}(\lambda) + J^{\mathcal{A}}_{\substack{\rm c,d\\ \rm in,d}}(\lambda) + J^{\mathcal{B}}_{\substack{\rm c,u\\ \rm in,d}}(\lambda). \end{aligned} \tag{10}$$

The functions on the right-hand side are given by

$$\begin{aligned} J^i_{\substack{l,\alpha\\ k,\beta}}(\lambda) &= \frac{\pi\left[T^2_{l,\alpha}\cdot I_i(\lambda, \tau_{\rm c}T_{l,\alpha}) - T^2_{k,\beta}\cdot I_i(\lambda, \tau_{\rm c}T_{k,\beta})\right]}{12}, \\ I_i(\lambda, a) &= \frac{6}{(\pi a)^2}\int_0^\infty \frac{dz z g_i(z,\lambda)}{\exp\left(\frac{z}{a}\right) - 1}, \quad i = \mathcal{A}, \mathcal{B}, \end{aligned} \tag{11}$$

where $g_{\mathcal{A}}(z,\lambda) = |iz + \lambda^2 - 1|^2/|(z+i)^2 + \lambda^2|^2$, $g_{\mathcal{B}}(z,\lambda) = \lambda^2 z^2/|(z+i)^2 + \lambda^2|^2$, and $z = \omega\tau_{\rm c}$ is the dimensionless integration variable. Note that the solution of Eq. (10) must be an even function of λ since $g_i(z, -\lambda) = g_i(z, \lambda)$.

We first concentrate on the limit of small temperatures $\max\{\tau_{\rm c}T_{l,\alpha}\} \ll 1$. In the case of ultimately strong coupling $\lambda = 1$, the system of equations simplifies, and to the leading order, one obtains equal temperatures:

$$T^2_{\rm c,u} = T^2_{\rm c,d} = \frac{T^2_{\rm in,u} + T^2_{\rm in,d}}{2}. \tag{12}$$

This result has a simple physical meaning: At $\lambda = 1$ and small temperatures, two ohmic contacts merge into one, and the total incoming heat flux $\pi(T^2_{\rm in,u} + T^2_{\rm in,d})/12$ is equally distributed between outgoing channels. In the case of weak coupling $\lambda \ll 1$, the equations in Eq. (10) can be expanded to include corrections to the leading order in λ:

$$\begin{aligned} T^4_{\rm c,u} &= T^4_{\rm in,u} + 2\lambda^2\left(T^4_{\rm in,d} - T^4_{\rm in,u}\right), \\ T^4_{\rm c,d} &= T^4_{\rm in,d} + 2\lambda^2\left(T^4_{\rm in,u} - T^4_{\rm in,d}\right). \end{aligned} \tag{13}$$

In the opposite limit of large temperatures, $\min\{\tau_{\rm c}T_{l,\alpha}\} \gg 1$, one arrives at the result that holds for arbitrary values of λ in the interval from 0 to 1 [37]:

$$\begin{aligned} T^2_{\rm c,u} &= T^2_{\rm in,u} + \frac{3\lambda^2(T_{\rm in,d} - T_{\rm in,u})}{2\pi\tau_{\rm c}}, \\ T^2_{\rm c,d} &= T^2_{\rm in,d} + \frac{3\lambda^2(T_{\rm in,u} - T_{\rm in,d})}{2\pi\tau_{\rm c}}. \end{aligned} \tag{14}$$

This is because, at large temperatures, the interactions are effectively weak for the arbitrary strength of coupling.

To investigate the thermal drag effect, we assume that the lower circuit is passive and cold $T_{\rm in,d} = 0$ and concentrate on the most interesting limit of low temperatures $\tau_{\rm c}T_{\rm in,u} \ll 1$. In the case of strong coupling $\lambda \to 1$, the temperatures of ohmic contacts are equal [see Eq. (12)]; therefore, the total incoming

heat flux $J_{\mathrm{in,u}} = J_{\mathrm{Q}}$ in the upper incoming channel with the temperature $T_{\mathrm{in,u}}$ splits into two equal outgoing fluxes. Thus, the thermal drag current in the lower circuit takes its maximum value of

$$J_{\mathrm{out,d}} = \frac{J_{\mathrm{in,u}}}{2}. \tag{15}$$

For small $\lambda \ll 1$, the the thermal drag current acquires the following form (see the Supplemental Material [37]):

$$J_{\mathrm{out,d}} = \frac{8\pi^2\lambda^2}{5}(\tau_{\mathrm{c}}T_{\mathrm{in,u}})^2 J_{\mathrm{in,u}}, \tag{16}$$

i.e., it is suppressed by two small parameters λ and $\tau_{\mathrm{c}}T_{\mathrm{in,u}}$. In what follows, we use Eqs. (15) and (16) to calculate the Fano factor of the thermal drag current noise.

IV. NOISE OF THERMAL DRAG CURRENT

The spectral density of heat current fluctuations at zero frequency and the Fano factor of the heat current are defined as

$$\mathcal{S}_{l,\alpha} = \int dt\,\langle \delta J_{l,\alpha}(t)\delta J_{l,\alpha}(0)\rangle, \quad F_{l,\alpha} \equiv \frac{\mathcal{S}_{l,\alpha}}{\langle J_{l,\alpha}\rangle}, \tag{17}$$

where $\delta J_{l,\alpha}(t) = J_{l,\alpha}(t) - \langle J_{l,\alpha}(t)\rangle$. We first consider an equilibrium ballistic channel at the temperature T as a reference. By substituting the operator of heat current from Eq. (9) into Eq. (17) and applying Wick's theorem, we arrive at the following result (see the Supplemental Material [37]) [35]:

$$\mathcal{S} = 2k_{\mathrm{B}}TJ_Q \equiv \mathcal{S}_{\mathrm{Q}} \quad \text{and} \quad F = 2k_{\mathrm{B}}T \equiv F_Q. \tag{18}$$

Thus, the upper incoming channel carries the heat current noise $\mathcal{S}_{\mathrm{in,u}} = \mathcal{S}_{\mathrm{Q}}$ with the temperature $T_{\mathrm{in,u}}$, and the Fano factor is equal to F_{Q}.

Next, using Eqs. (6) and (7), after some algebra, we arrive at the following expression:

$$\mathcal{S}_{\mathrm{out,d}} = \sum_{\substack{lk\\ \alpha\beta}} \int \frac{d\omega}{2\pi} S_{l,\alpha}(-\omega)\mathcal{M}_{l,\alpha;k,\beta}(-\omega,\omega)S_{k,\beta}(\omega), \tag{19}$$

where $S_{l,\alpha}(\omega)$ are given in Eq. (8), and we introduced $\mathcal{M}_{l,\alpha;k,\beta}(-\omega,\omega) = m_{l,\alpha}(-\omega)m_{k,\beta}(\omega)/2$ with $m_{\mathrm{in,u}}(\omega) = |\mathcal{B}(\omega)|^2$, $m_{\mathrm{in,d}}(\omega) = |\mathcal{A}(\omega)|^2$, $m_{\mathrm{c,d}}(\omega) = |\mathcal{C}(\omega)|^2$, and $m_{\mathrm{c,u}}(\omega) = m_{\mathrm{in,u}}(\omega)$. This general result can be applied to a number of physical situations. Below, we concentrate on the noise of the thermal drag current in the most interesting limit of $T_{\mathrm{in,d}} = 0$ and $\tau_{\mathrm{c}}T_{\mathrm{in,u}} \ll 1$ and in the regimes of strong and weak coupling.

In the limit $\lambda = 1$, one can set $m_{\mathrm{in,u}} = m_{\mathrm{in,d}} = m_{\mathrm{c,u}} = m_{\mathrm{c,d}} = \frac{1}{4}$, and the straightforward calculation gives (see the Supplemental Material [37])

$$\mathcal{S}_{\mathrm{out,d}} = \frac{3\mathcal{I}}{2\pi^2}\mathcal{S}_{\mathrm{in,u}}, \tag{20}$$

where $\mathcal{I} \approx 2.5782$. By using the expression for heat current in the lower outgoing channel, Eq. (15), we obtain the Fano factor of the thermal drag current:

$$\frac{F_{\mathrm{out,d}}}{F_{\mathrm{in,u}}} \approx 1.5673. \tag{21}$$

In the limit of weak coupling $\lambda \ll 1$, one obtains (see the Supplemental Material [37])

$$\mathcal{S}_{\mathrm{out,d}} = \frac{3\lambda^2\mathcal{K}}{2}(\tau_{\mathrm{c}}T_{\mathrm{in,u}})^2\mathcal{S}_{\mathrm{in,u}}, \tag{22}$$

where $\mathcal{K} \approx 10$. By using Eq. (16) for the heat current, one obtains the Fano factor:

$$\frac{F_{\mathrm{out,d}}}{F_{\mathrm{in,u}}} \approx 0.9498. \tag{23}$$

The above result deserves an additional discussion. First, we note that the Fano factor of the noise of the equilibrium heat current can be estimated as a size of the typical fluctuation of heat, which is of the order of the average heat current times the correlation time. In equilibrium, the correlation time of the heat current noise is of the order of $1/T$ (the only available timescale). That is why the Fano factor of the equilibrium heat current noise scales linearly with the temperature [see Eq. (18)]. Therefore, it appears somewhat surprising, from the first glance, that in the weak coupling regime $\lambda \ll 1$, the Fano factor of the thermal drag current is close to the one of the incoming equilibrium channel with the temperature $T_{\mathrm{in,u}}$, despite the fact that the effective temperature of the thermal drag current scales as $\lambda\tau_{\mathrm{c}}T_{\mathrm{in,u}}^2$, i.e., it is smaller by the dimensionless factor $\lambda\tau_{\mathrm{c}}T_{\mathrm{in,u}} \ll 1$. The explanation of this effect lies in the fact that, in the weak coupling regime, the thermal drag effect can be viewed as essentially a nonequilibrium rare Poissonian process of the emission and reabsorption of photons between the upper and lower parts of the circuit. In this case, the Fano factor acquires the values of the order of the average energy of transmitted photons, which is of the order of the temperature of the incoming equilibrium channel.

To summarize, we have proposed and theoretically analyzed a strongly interacting mesoscopic electron system for studying the thermal drag effect. The system that is based on QH edge states perfectly coupled to ohmic contacts is accessible to modern experiments. It consists of an active circuit, where the heat is generated, and a passive circuit, where the heat flux is induced by nonlocal Coulomb interactions. The model of the system is exactly integrable with the help of the bosonization technique and the scattering theory for bosons. We have calculated the thermal drag current, the corresponding zero frequency noise power, and the Fano factor of the thermal noise. It has been shown that, depending on the interaction strength, the Fano factor can be larger or smaller than the Fano factor of the equilibrium ballistic channel.

ACKNOWLEDGMENTS

E.G.I. acknowledges financial support from the National Research Fund Luxembourg under Grant No. CORE C19/MS/13579612/HYBMES. E.V.S. acknowledges financial support from the Swiss National Science Foundation.

[1] B. N. Narozhny and A. Levchenko, Rev. Mod. Phys. **88**, 025003 (2016).

[2] A. Levchenko and A. Kamenev, Phys. Rev. Lett. **101**, 216806 (2008).

[3] O. E. Raichev, G. M. Gusev, F. G. G. Hernandez, A. D. Levin, and A. K. Bakarov, Phys. Rev. B **102**, 195301 (2020).

[4] J. H. Strait, G. Holland, W. Zhu, C. Zhang, B. R. Ilic, A. Agrawal, D. Pacifici, and H. J. Lezec, Phys. Rev. Lett. **123**, 053903 (2019).

[5] V. L. Gurevich and M. I. Muradov, J. Exp. Theor. Phys. **121**, 998 (2015).

[6] P. Ben-Abdallah, S. A. Biehs, and K. Joulain, Phys. Rev. Lett. **107**, 114301 (2011).

[7] B. Bhandari, G. Chiriacò, P. A. Erdman, R. Fazio, and F. Taddei, Phys. Rev. B **98**, 035415 (2018).

[8] P. Ben-Abdallah, Phys. Rev. B **99**, 201406(R) (2019).

[9] W. Berdanier, T. Scaffidi, and J. E. Moore, Phys. Rev. Lett. **123**, 246603 (2019).

[10] D. Venturelli, R. Fazio, and V. Giovannetti, Phys. Rev. Lett. **110**, 256801 (2013).

[11] Y. Zhang, G. Lin, and J. Chen, Phys. Rev. E **91**, 052118 (2015).

[12] J. V. Koski, V. F. Maisi, J. P. Pekola, and D. V. Averin, Proc. Natl. Acad. Sci. USA **111**, 13786 (2014).

[13] R. S. Whitney, R. Sánchez, F. Haupt, and J. Splettstoesser, Phys. E **75**, 257 (2016).

[14] T. Ruokola and T. Ojanen, Phys. Rev. B **83**, 241404(R) (2011).

[15] D. Sánchez and M. Moskalets, Entropy **22**, 977 (2020).

[16] Z. Iftikhar, *Charge Quantization and Kondo Quantum Criticality in Few-Channel Mesoscopic Circuits*, 1st ed. (Springer International Publishing, Cham, 2018).

[17] S. Jezouin, F. D. Parmentier, A. Anthore, U. Gennser, A. Cavanna, Y. Jin, and F. Pierre, Science **342**, 601 (2013).

[18] S. Jezouin, Z. Iftikhar, A. Anthore, F. D. Parmentier, U. Gennser, A. Cavanna, A. Ouerghi, I. P. Levkivskyi, E. Idrisov, E. V. Sukhorukov *et al.*, Nature (London) **536**, 58 (2016).

[19] E. G. Idrisov, I. P. Levkivskyi, and E. V. Sukhorukov, Phys. Rev. B **96**, 155408 (2017).

[20] A. Furusaki and K. A. Matveev, Phys. Rev. B **52**, 16676 (1995).

[21] A. O. Slobodeniuk, I. P. Levkivskyi, and E. V. Sukhorukov, Phys. Rev. B **88**, 165307 (2013).

[22] E. Sivre, A. Anthore, F. D. Parmentier, A. Cavanna, U. Gennser, A. Ouerghi, Y. Jin, and F. Pierre, Nat. Phys. **14**, 145 (2018).

[23] A. A. Clerk, P. W. Brouwer, and V. Ambegaokar, Phys. Rev. Lett. **87**, 186801 (2001).

[24] E. G. Idrisov, I. P. Levkivskyi, and E. V. Sukhorukov, Phys. Rev. Lett. **121**, 026802 (2018).

[25] H. Duprez, E. Sivre, A. Anthore, A. Aassime, A. Cavanna, U. Gennser, and F. Pierre, Science **366**, 1243 (2019).

[26] Z. Iftikhar, S. Jezouin, A. Anthore, U. Gennser, F. D. Parmentier, A. Cavanna, and F. Pierre, Nature (London) **526**, 233 (2015).

[27] Z. Iftikhar, A. Anthore, A. K. Mitchell, F. D. Parmentier, U. Gennser, A. Ouerghi, A. Cavanna, C. Mora, P. Simon, and F. Pierre, Science **360**, 1315 (2018).

[28] M. Banerjee, M. Heiblum, A. Rosenblatt, Y. Oreg, D. E. Feldman, A. Stern, and V. Umansky, Nature (London) **545**, 75 (2017).

[29] M. Banerjee, M. Heiblum, V. Umansky, D. E. Feldman, Y. Oreg, and A. Stern, Nature (London) **559**, 205 (2018).

[30] D. F. Mross, Y. Oreg, A. Stern, G. Margalit, and M. Heiblum, Phys. Rev. Lett. **121**, 026801 (2018).

[31] W. Pouse, L. Peeters, C. L. Hsueh, U. Gennser, A. Cavanna, M. A. Kastner, A. K. Mitchell, and D. Goldhaber-Gordon, arXiv:2108.12691 (2022).

[32] X. G. Wen, Phys. Rev. B **41**, 12838 (1990).

[33] T. Giamarchi, *Quantum Physics in One Dimension* (Clarendon Press, Oxford, 2003).

[34] E. M. Lifshitz and L. P. Pitaevskii, *Statistical Physics, Part 2: (Landau and Lifshits Course of Theoretical Physics, Vol. 9)* (Butterworth-Heinemann, Oxford, 1980).

[35] J. P. Pekola and B. Karimi, Rev. Mod. Phys. **93**, 041001 (2021).

[36] A. Rosenblatt, S. Konyzheva, F. Lafont, N. Schiller, J. Park, K. Snizhko, M. Heiblum, Y. Oreg, and V. Umansky, Phys. Rev. Lett. **125**, 256803 (2020).

[37] See Supplemental Material at http://link.aps.org/supplemental/10.1103/PhysRevB.106.L121405 for the detailed calculations of temperature, heat current, and corresponding noise.